Ultrasonic fatigue testing of AISI 304 and 316 stainless steels under environmental and immersion conditions

Luis M. Torres Duarte, Gonzalo M. Domínguez Almaraz, Hipólito M. Venegas Montaño
University of Michoacán (UMSNH), Faculty of Mechanical Engineering, Santiago Tapia 403, Col. Centro, Morelia, 58000, Mexico
lmtorres@umich.mx
dalmaraz@umich.mx, https://orcid.org/0000-0002-8786-8640
0468633k@umich.mx

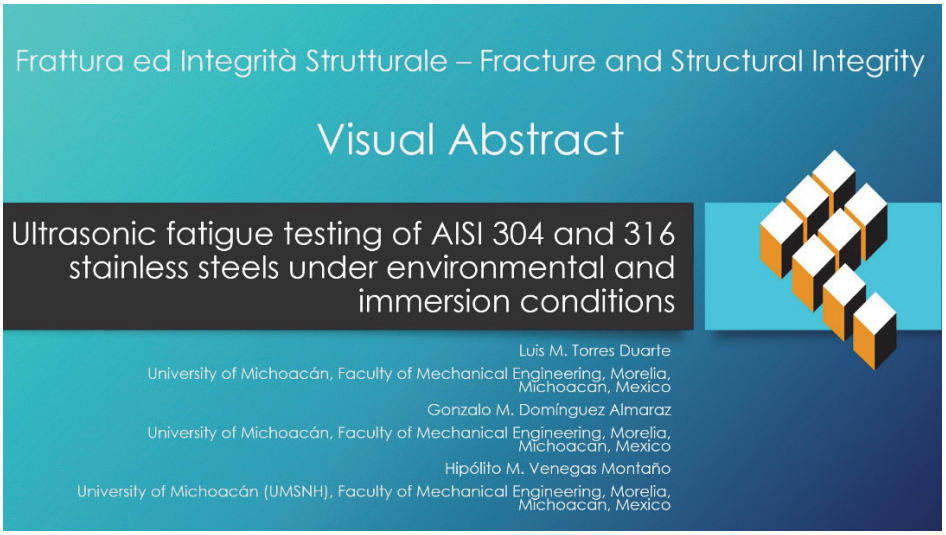

Citation: Torres Duarte, L. M., Domínguez Almaraz, G. M., Venegas Montaño, H. M., Ultrasonic fatigue testing of AISI 304 and 316 stainless steels under environmental and immersion conditions, Frattura ed Integrità Strutturale, 68 (2024) 175-185.

Received: 28.10.2023
Accepted: 05.01.2024
Published: 28.01.2024
Issue: 01.04.2024

KEYWORDS. Ultrasonic fatigue tests, Stainless steels, Immersion, Crack Propagation, Fatigue life.

INTRODUCTION

For decades stainless steel has been of great importance due to its wide range of applications; which can span from common to advanced industrial uses. Some of their uses include architectural structures, marine systems, chemical industry, food industry, medical devices, nuclear applications, petroleum industry, airplanes and aerospace, among the most significant. These applications often involve mechanical and physical factors, such as: fatigue load, temperature, and environmental conditions… that can be crucial for proper functioning across various industrial applications, including those mentioned above [1-4]. Some stainless steels have special properties, as is the case with austenitic steels that exhibit non-magnetic properties [1, 3-4]. Among the most common types of austenitic stainless steels are the designated AISI 316

and 304, which contain elements such as chromium (Cr), nickel (Ni), manganese (Mn), and molybdenum (Mo), significantly enhancing their resistance to corrosive attacks [5,6]. Chromium forms a passive film that protects the stainless-steel surface, while the inclusion of molybdenum (present in stainless steel 316), reinforces corrosion resistance under more extreme conditions, reducing deterioration of the passive surface film [7,8].

Due to the multiple physical and mechanical properties of these materials, a wide variety of studies have been carried out in different fields: Di W. et al. [5] investigated the effect of microbiological agents as corrosion generators on stainless steel 304 and 316, reporting better corrosion resistance in stainless steel 316. Research has also been carried out on stainless steel 316L, as mentioned by Seong-Gu H. and Soon-Bok L. [9], who conducted fatigue tests at low frequencies and temperatures ranging from 20 to 750 °C, observing a significant decrease in fatigue strength at high temperatures. Chao H. et al. [10] performed tests on the ultrasonic fatigue damage behavior of stainless steel 304L, reporting slip marks (micro-plasticity) on the surface of the specimen along with a heat dissipation process before failure. A. Grigorescu et al. [11] studied the behavior of stainless steels 304L, 316L, and 904L in the HCF and VHCF regimes, explaining the fatigue life cycles of each under different loading conditions, considering their chemical and mechanical properties. Other studies, such as the one by Ludovic V. et al. [12], have focused on stainless steel 304L under high fatigue cycles: they conducted tests at room temperature on stainless steel 304L from different suppliers, controlling the stress amplitude between 180 MPa and 210 MPa and the strain between 0.17% and 0.5%. Among their findings, they highlighted that the martensitic transformation phase and secondary hardening at room temperature are related to high fatigue cycles. Kyouhei T. and Takeshi O. [13], carried out ultrasonic fatigue tests to evaluate the fatigue properties of stainless steel in the SUS316NG and SUS304 grades according to the Japan Industrial Standards; they subjected the material to pre-deformation in tension (5%, 10%, and 20%) and compression (-20%) before machining the specimens. To prevent heating during ultrasonic fatigue tests, the specimens were placed in a low-temperature chamber (-100 °C), and the loading condition was intermittent. Jan K. et al. [14,15] conducted experiments to study the fatigue behavior of stainless steels 1.4306 and 1.4307 (316L). They observed that steel 1.4306 exhibited greater strength than 1.4307 and reported failure in the range below 1×106 cycles (HCF) and between 1x107 and 1×109 cycles (VHCF) for specimens subjected to loads of 270 and 280 MPa. For steel 1.4306, failure was not observed in the VHCF regime.

In the current study specimens were tested at room temperature and under immersion conditions (water and antifreeze). Despite the close resemblance of 316 and 304 stainless steels with those mentioned earlier, they possess slightly different properties. Then, the obtained results are presumed to be novel since the applied cooling conditions in the present study differ from those reported in the consulted literature.

MATERIALS AND EXPERIMENTAL PROCEDURES.

Stainless steel denomination AISI 316 and 304 were acquired from the company "La Paloma Compañía de Metales S.A. de C.V." (Morelia Michoacán, México), whose chemical composition by weight is shown in Tab. 1, and the main mechanical properties are listed in Tab. 2. The bars were obtained with a diameter of 12.7 mm (1/2 inch). All specimens were tested with a loading ratio R = -1.

Name	C	Cr	Ni	Mn	Si	P	S	other elements
316	0.08 max.	18-20	8-11	2 max.	1 max.	0.04 max.	0.03 max.	
304	0.08 max.	16-18	10-14	2 max.	1 max.	0.04 max.	0.03 max.	Mo. 2-3

Table 1: Chemical composition of the AISI 316 and 304 austenitic stainless steels (in % mass) [16,17].

Name	Young's modulus (GPa)	Density (kg/m^3)	Poisson ratio	Tensile strength (MPa)	0.2% Offset Yield Stress (MPa)
316	193	8027	0.30	580	289.6
304	193	8927	0.30	580.	276

Table 2: Main mechanical properties of the AISI 316 and 304 austenitic stainless steels [16,17].

MODELING AND NUMERICAL SIMULATION.

The design of the specimens must comply with the resonance conditions of the ultrasonic fatigue machine, which has a working frequency of 20 kHz ± 200 Hz. Therefore, it is important to perform numerical simulations that ensure that one of the natural frequency modes, specifically in the longitudinal direction of the specimen, is close to the machine work value. A 3D model was created using SolidWorks software to later export it to ANSYS Workbench (AW) with the ".STEP" extension. Dimension of specimen are obtained by Finite Element Modal Analysis using the mechanical properties of material (Elastic Modulus, density and Poisson ratio), and modifying the length of specimen in the constant diameter section to fit the resonance conditions. In Fig. 1 are illustrated the final dimensions of the ultrasonic fatigue specimens 304 and 316, fitting the resonance conditions.

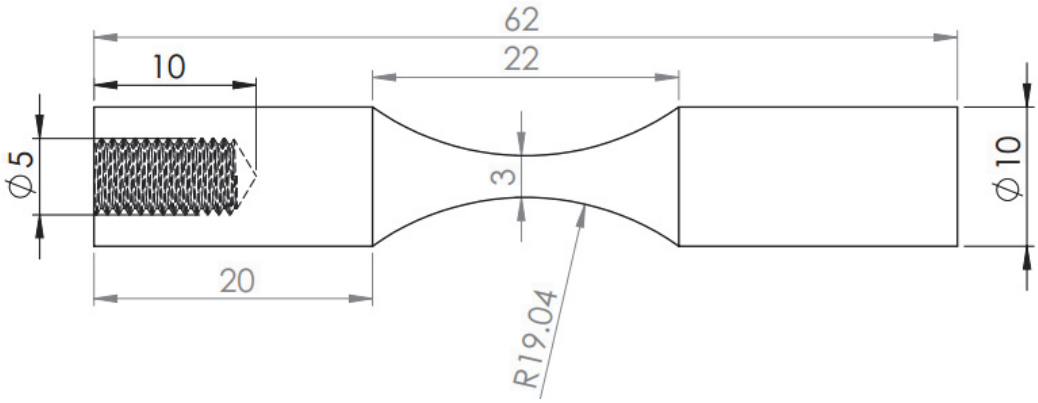

Figure 1: Final dimensions (mm), of ultrasonic fatigue specimen for AISI 304 and 316 stainless steels.

In Tab. 3 are listed the main properties of the mesh used in the modal analysis. The numerical simulation was performed to obtain the first 16 modes of vibration; Tab. 4 shows the frequencies of the natural vibration modes of this specimen, with mode number 12 corresponding to the longitudinal vibration of specimen with 19,999 Hz. The longitudinal mode of vibration of testing specimens were obtained using numerical modal analysis, as presented in Fig. 2, where the natural frequency of vibration in longitudinal direction was 19,999 Hz.

Element type	Element size	Elements	Nodes
SOLID 185	0.001 m	9984	43055

Table 3: Main properties of the mesh used in modal simulation.

Mode	1-4	5	6	7-8	9	10	11	12	13-14	15-16
Frequency (Hz)	0	6.65×10^{-3}	3.32×10^{-2}	2474.3	4817.5	14435	14435	19999	50131	60333

Table 4: First 16 Frequency Modes of the specimen.

After obtained the specimen dimensions by modal numerical analysis, specimens were machined obtaining the profile showed in Fig. 3a. Afterwards, the specimen was mounted in the ultrasonic fatigue machine, Fig. 3b, in order to verify the required condition of resonance vibration.

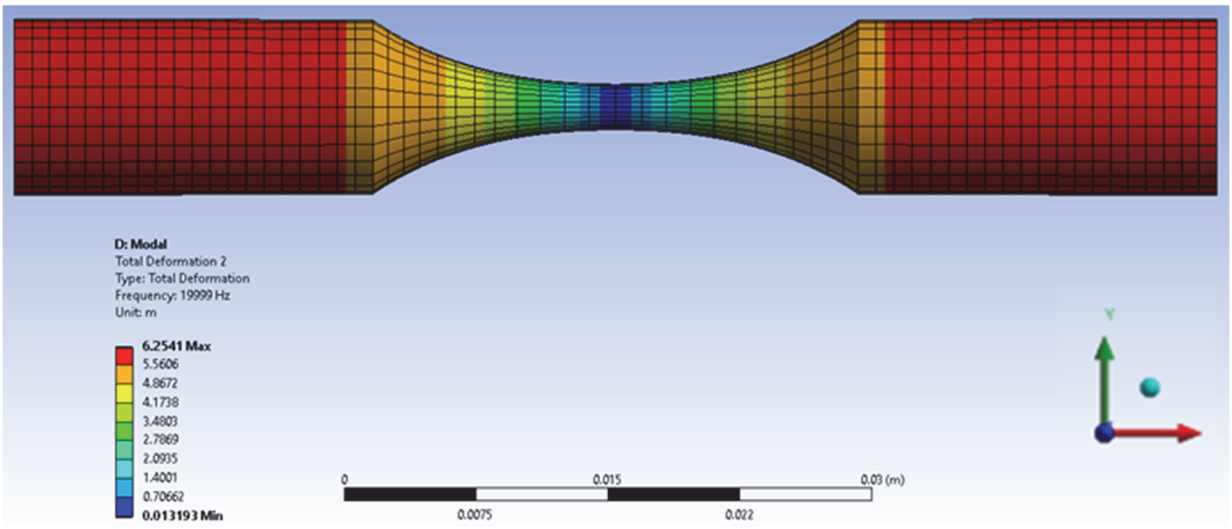

Figure 2: Longitudinal vibration mode of the specimen close to 20KHz.

Figure 3: a) Machined specimen, and b) Specimen mounted in the ultrasonic machine.

Additional numerical simulations were conducted to obtain the stresses distribution along the narrow section of specimen. The ultrasonic fatigue machine operates based on displacements generated by voltage values: one volt corresponds to 0.7 micrometers of displacement, and the lowest operating voltage of the machine is 10 volts, which translates a displacement of 7 micrometers. The conditions imposed in the simulation were as follows: fixing one end of the specimen and applying a displacement to the other end. Tab. 5 presents the main mesh properties for this simulation, and Fig. 4 depicts the simulation procedure for obtaining the stresses distribution along the narrow section of the specimen when it is subjected to a displacement of 7 μm.

Element type	Element size	Elements	Nodes
Default	0.0005 m	326246	78720

Table 5: General characteristics of the mesh used for load condition.

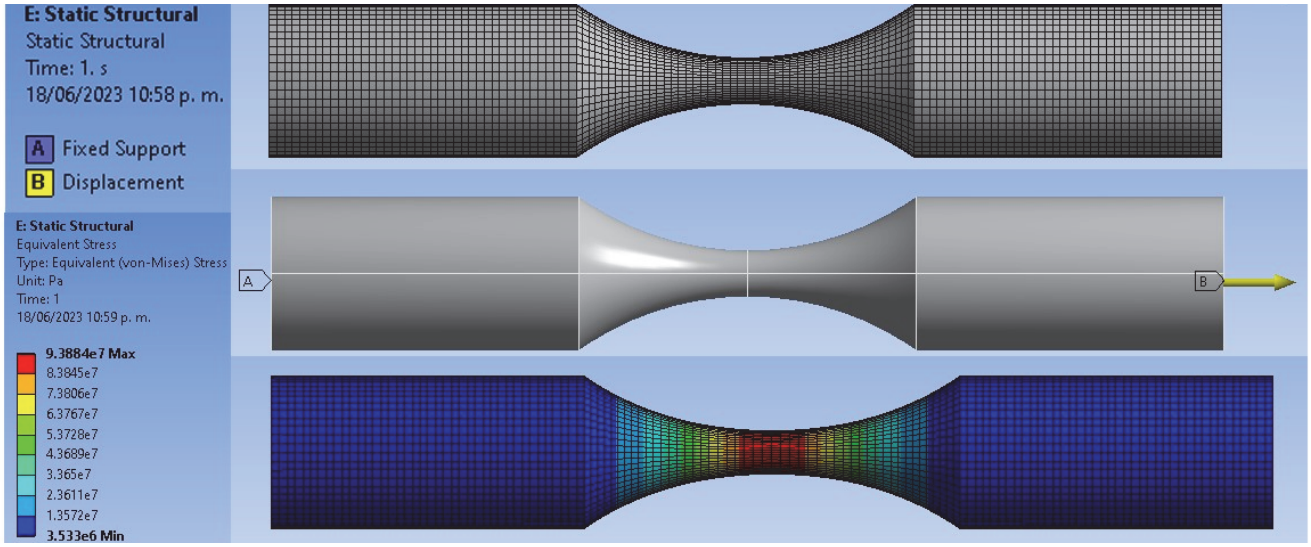

Figure 4: Numerical simulation to obtain the stresses generated with 7 μm of displacement.

The simulation results revealed that applying a displacement of 7 μm to the specimen generates an approximate stress of 94 MPa in its narrow section. As this value falls within the elastic range, linear behavior is considered. Other linear values are listed in Tab. 6, following the linear relationship between voltage – displacement at the free end – stress.

Voltage (v)	Displacement (μm)	Stress (Pa)	Total deformation (m)	% of yield stress of 316 (289.6 MPa)	% of yield stress of 304 (276 MPa)
10	7	9.39×10^{7}	7.00×10^{-6}	32.42	34.02
12	8.4	1.13×10^{8}	8.40×10^{-6}	38.90	40.82
14	9.8	1.31×10^{8}	9.80×10^{-6}	45.39	47.62
16	11.2	1.50×10^{8}	1.12×10^{-5}	51.87	54.42
18	12.6	1.69×10^{8}	1.26×10^{-5}	58.35	61.23
20	14	1.88×10^{8}	1.40×10^{-5}	64.84	68.03
21	14.7	1.97×10^{8}	1.47×10^{-5}	68.08	71.43
22	15.4	2.07×10^{8}	1.54×10^{-5}	71.32	74.84
23	16.1	2.16×10^{8}	1.61×10^{-5}	74.56	78.24
24	16.8	2.25×10^{8}	1.68×10^{-5}	77.80	81.64
25	17.5	2.35×10^{8}	1.75×10^{-5}	81.05	85.04
26	18.2	2.44×10^{8}	1.82×10^{-5}	84.29	88.44
27	18.9	2.53×10^{8}	1.89×10^{-5}	87.53	91.84
28	19.6	2.63×10^{8}	1.96×10^{-5}	90.77	95.24

Table 6: Linear relationship between Voltage-Displacement-Stress.

EXPERIMENTAL RESULTS

Ultrasonic fatigue tests were conducted on stainless steel 316 and 304 under two modalities: at room temperature and under immersion conditions. Stainless steel 316 was immersed in water, while stainless steel 304 was immersed in antifreeze.

In tests conducted at room temperature in both denominations of stainless steel, it was not possible to establish a clear ultrasonic fatigue behavior pattern. This can be attributed to the poor heat dissipation properties of stainless steels,

characterized by their low thermal conductivity coefficient (16.2 W/m *K),* in comparison to other materials such as aluminum *(205-240 W/m K)*. First tests in this condition were conducted with loads of 188 MPa and 197 MPa, revealing high temperature recorded by FLIR i7 thermal camera, Fig. 5a, and affecting thermally the specimen at the neck section, Fig. 5b. However, it is assumed that these values could be higher since they are captured just before visible heating, a characteristic that is associated with thermal failure. The infrared camera captured this effect before reaching the maximum instantaneous temperature. For loads exceeding the mentioned levels, the effect remained consistent and even faster.
By decreasing the load to values of 170 MPa, the thermal effect became less pronounced, and the material did not fracture. Thus, owing to the low stress applied to the material, the fatigue life under these conditions may be considered infinite, with values reaching up to 6.31×10^{11} cycles without failure.

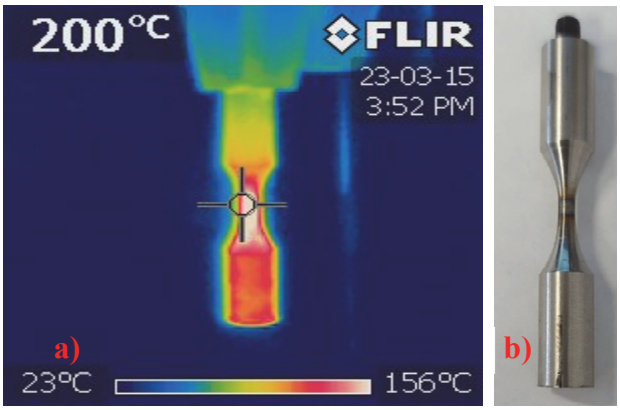

Figure 5: a) Temperature recorded in specimens before failure, b) Thermal effect in specimen tested at room temperature.

On the other hand, the temperature effect for ultrasonic fatigue tests on stainless steel 316 immersed in water was significantly reduced, since the measured temperature remained below 100 °C. Under this condition, the fatigue life behavior for this material was established under different load levels. Fig. 6 illustrates the arrangement for testing with a 316 stainless steel specimen immersed in water as well as the temperature recorded during the test. Tests were carried out with different load levels: ranging from 188 MPa to 263 MPa. The voltage increment criterion was set, which consisted of raising the voltage by 1 volt (approximately equivalent to 13.4 MPa), every 10 seconds until reaching the specified value for each test. Tab. 7 presents the results obtained in ultrasonic fatigue for the different load levels defined for the immersed stainless steel 316.

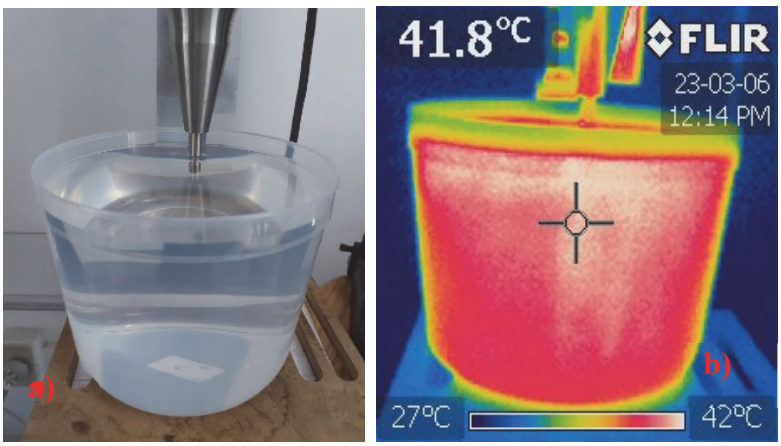

Figure 6: a) 316 stainless steel specimen immersed in water, b) Temperature recorded during the test.

Fig. 7 shows a graph of the behavior of 316 stainless steel, stress vs number of cycles. A linear trend line is displayed to represent the fatigue behavior of 316 stainless steel immersed in water.
Concerning ultrasonic fatigue tests of stainless steel 304 under immersion conditions, a BARDAHL 50/50 antifreeze with a boiling point of 132 °C was used. Under this modality, the temperature effect was also reduced. However, unlike water immersion tests, the use of antifreeze led to a reduction in potential corrosive effects on the specimens. This is attributed

to the fact that in some specimens immersed in water, corrosive effects were observed due to water contact and the high operational frequency of the machine.

Stress (MPa)	Voltage (v)	Test time (s)	Number of cycles
187.8	20	594000	1.19×10^{10}
197.2	21	135	2.70×10^{6}
206.5	22	1860	3.72×10^{7}
206.5	22	661.8	1.32×10^{7}
206.5	22	1411.8	2.82×10^{7}
215.9	23	828.6	1.66×10^{7}
215.9	23	210	4.20×10^{6}
215.9	23	702.6	1.40×10^{7}
225.3	24	948	1.90×10^{7}
225.3	24	826.8	1.65×10^{7}
234.7	25	255.6	5.11×10^{6}
234.7	25	927.6	1.86×10^{7}
244.1	26	300	6.00×10^{6}
253.5	27	175.2	3.51×10^{6}
253.5	27	210	4.2×10^{6}
253.5	27	310.02	6.20×10^{6}
262.9	28	375	7.50×10^{6}
262.9	28	350.4	7.00×10^{6}

Table 7: Ultrasonic fatigue experimental data obtained for 316 stainless steel specimens immersed in water.

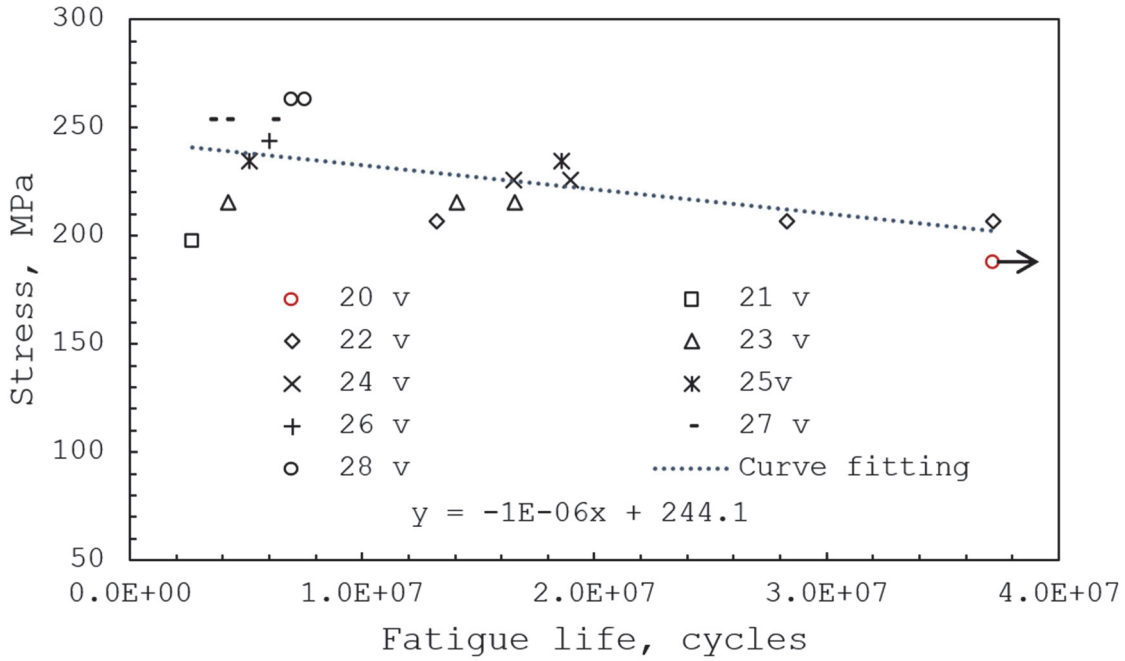

Figure 7: Stress-number of cycles graph of 316 stainless steel immersed in water, with representative marks of the used voltages.

In Tab. 8 are listed the experimental tests performed on stainless steel 304 immersed in antifreeze. At the lowest working load of 169 MPa, specimens exhibited a fatigue life exceeding 3.44×10^{9} cycles; while tests conducted at the highest load (263 MPa) demonstrated a fracture for 3.62×10^{6} cycles. Fig. 8 displays the stress-number of cycles graph illustrating the ultrasonic fatigue behavior of stainless steel 304 immersed in antifreeze.

Stress (MPa)	Voltage (v)	Test time (s)	Number of cycles
169	18	172152	3.44×10^{9}
178.4	19	54972	1.10×10^{9}
178.4	19	97200	1.94×10^{9}
187.8	20	10158	2.03×10^{8}
197.20	21	4824	9.65×10^{7}
206.50	22	7945.2	1.59×10^{8}
215.90	23	3555.6	7.11×10^{7}
225.30	24	189.9	3.80×10^{6}
234.70	25	82	1.64×10^{6}
244.10	26	95.6	1.91×10^{6}
262.90	28	181.2	3.62×10^{6}

Table 8: Ultrasonic fatigue experimental data obtained for 304 stainless steel specimens immersed in antifreeze.

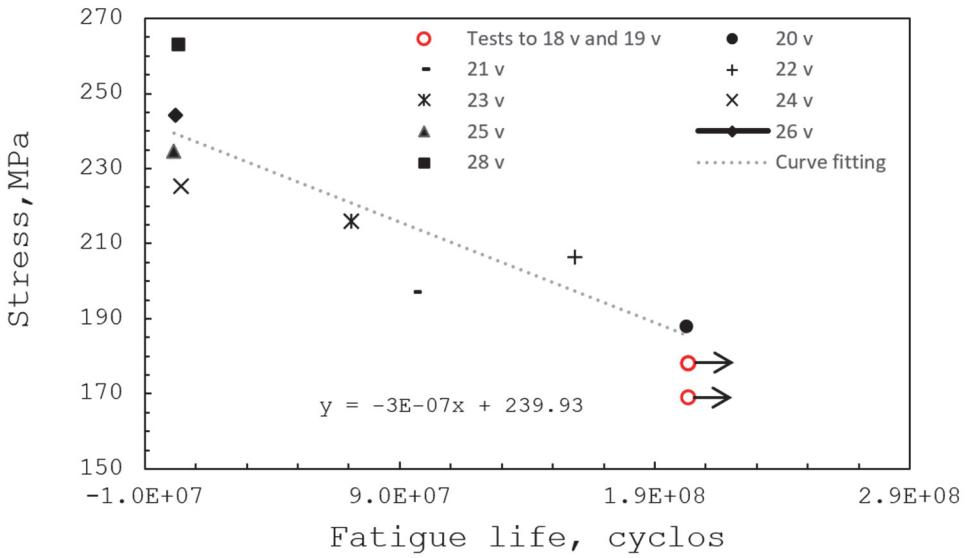

Figure 8: Stress-number of cycles graph of 304 stainless steel immersed in antifreeze.

Discussion

Results obtained from the tests conducted on stainless steel 316 and 304 at room temperature revealed that at loads higher than 188 MPa, the thermal effect is a decisive factor in specimen fracture, rapidly occurring when the temperature exceeds 200 °C. However, by reducing the load to values below 170 MPa, the thermal effect becomes less damaging, and the temperature remains below 190 °C. With these load values, the specimen did not fracture even after 6.31×10^{11} cycles.

Fig. 9 displays scanning electron microscopy visualizations of stainless steel 316 and 304 at a load of 188 MPa under room temperature conditions. The cause of failure was due to the thermal effect at the edge of the specimen surface, which subsequently combined with typical mechanical failure behavior. An image magnification was conducted in the thermally affected zone, revealing alterations in the granular scale of the material. In the stainless steel 316 specimens a corona was observed between the thermally affected zone and the mechanical crack propagation zone.

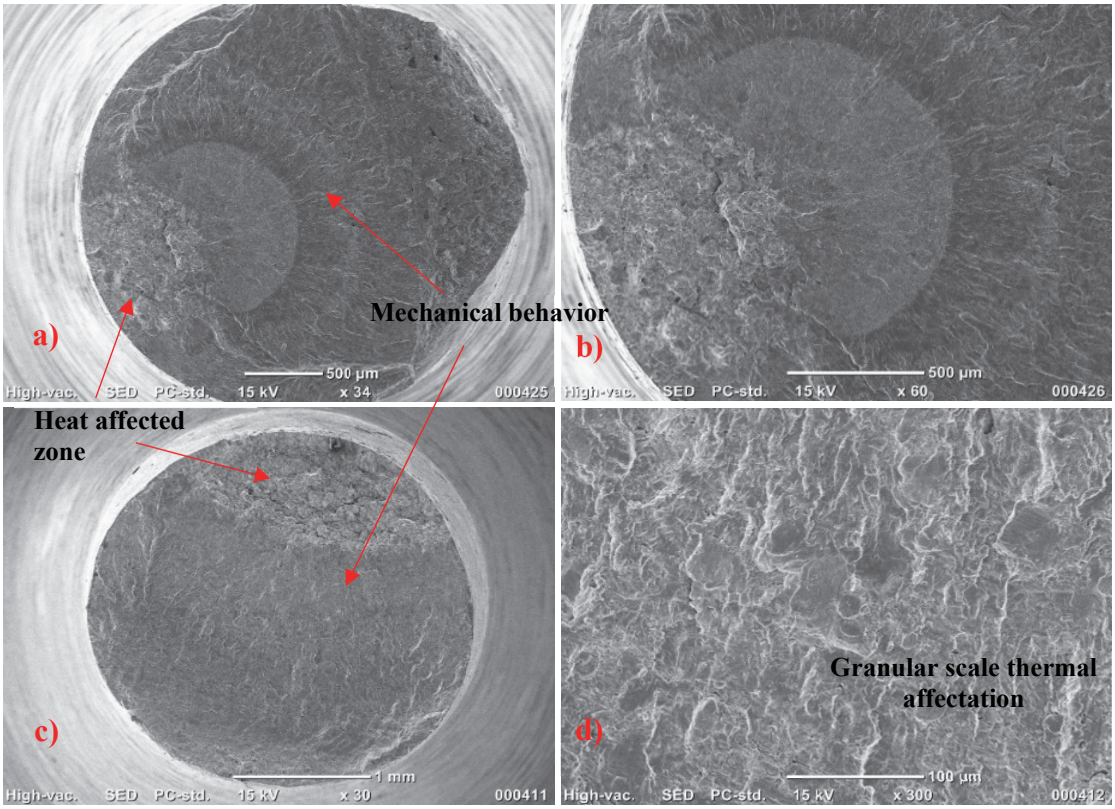

Figure 9: Inspection of fracture zones using SEM (Scanning Electron Microscopy) in specimens at 20 v: a) and b), stainless steel 316; c) and d), stainless steel 304.

Tests in immersion conditions provided information about the behavior pattern of stainless steel 316 and 304; where the 316 subjected to the highest load (263 MPa), exhibited a fatigue life of 7×10^6 cycles before failure; whereas the 304 displayed a fatigue life of 3.6×10^6 cycles under the same loading conditions. For lower loads on stainless steel 316, a load of 188 MPa was employed, resulting in a fatigue life of 1.2×10^{10} cycles before failure. Furthermore, the lowest load for the 304 was 169 MPa, resulting in values that exceed the 3.44×10^9 cycles of fatigue life. With the previous results, it can be deduced that stainless steel 316 exhibits greater resistance to ultrasonic fatigue compared to stainless steel 304, under immersion conditions. However, it is crucial to note that the immersion fluid was distinct for each denomination.

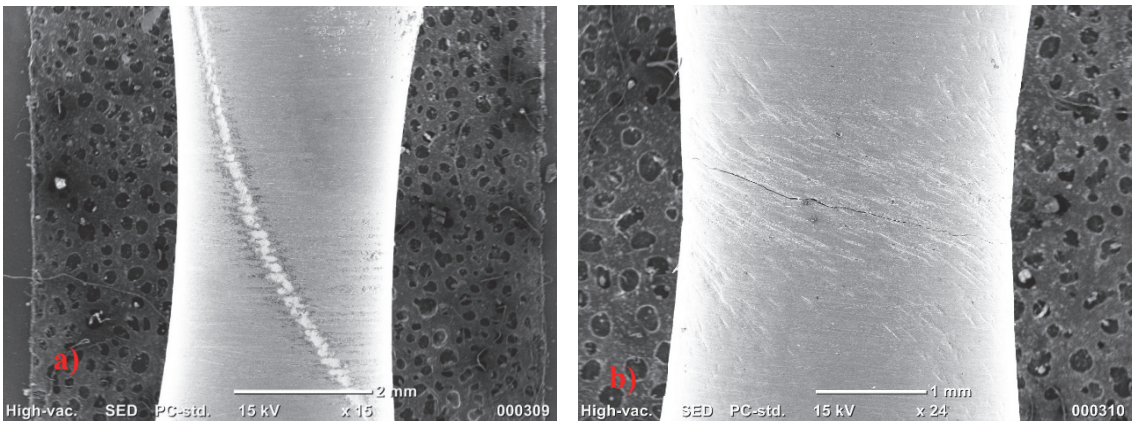

Figure 10: Corrosion wear on the surface of the specimens immersed in water. a) specimen at 20 volts in immersion after 165 hours in ultrasonic fatigue and b) specimen at 21 volts.

The kind of cooling fluid for ultrasonic fatigue tests plays a significant role, as evidenced by tests on stainless steel 316 immersed in water, in which wear on the surface of the narrow section of the specimens was observed, as depicted in Fig.

10. This effect was not observed in the stainless steel 304 specimens immersed in antifreeze, a fluid that has anticorrosive properties. Although stainless steel 316 has better anticorrosive properties than 304, ultrasonic fatigue tests with immersion in water exhibited an increased corrosive effect compared to stainless steel 304 immersed in antifreeze.
The initiation and propagation of the crack, for both stainless steel 316 and 304, originated on the surface of the narrow section of the specimen, as illustrated in Fig. 11. Furthermore, for specimens immersed, crack initiation and propagation exhibit a typical mechanical behavior, without any apparent thermal affectation.

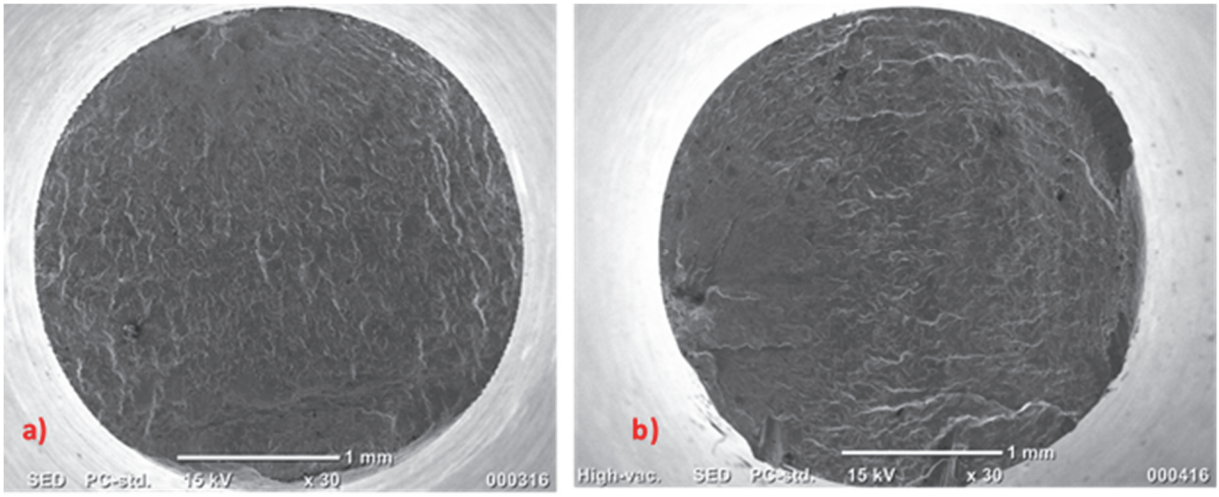

Figure 11: Fracture surfaces and crack initiation and propagation. a) 316 stainless steel specimen immersed in water, b) 304 stainless steel specimen immersed in antifreeze.

Since the fracture was initiated on the specimen surface, a roughness analysis was performed to ascertain the Ra values of the machined specimens. An average value below 0.5 μm was obtained, which is within the high-demand criteria requested for fatigue applications.

CONCLUSIONS

The following conclusions can be drawn from the present work:

- Tests were carried out at room temperature on stainless steel AISI 304 and 316 revealed that, with loads of 188 MPa, material failure occurs rapidly due to the thermal effect, exceeding temperatures of 200 °C.
- For loads equal to or less than 170 MPa, the results obtained at room temperature for both materials show that the thermal effect does not exceed 190°C, and failure does not occur after 6.31×10^{11} cycles.
- Tests on stainless steel 316 immersed in water under loads of 263 MPa exhibited a fatigue life of 7×10^{6} cycles before failure, while tests at 188 MPa loads showed a lifetime of 1.2×10^{10} cycles before failure.
- Results obtained for stainless steel 304 immersed in antifreeze indicated a fatigue life of 3.6×10^{6} cycles under 263 MPa loads. However, when subjected to loads of 169 MPa, the lifetime increased to 3.44×10^{9} cycles before failure.
- For both stainless steels, crack initiation and propagation occurred on the surface of the specimens. In tests conducted at room temperature, failure initiation was due to the thermal effect, causing grain-level alteration, which later combined with typical mechanical failure behavior. In the case of immersion tests, failure occurred with visibly mechanical behavior and crack initiation at the surface.
- The surface finish of the specimen plays a crucial role as the failure originates at the surface. Therefore, proper polishing or surface treatment of the specimens can improve the fatigue life of the material under ultrasonic fatigue testing. The roughness coefficient Ra measured on the specimens of stainless steel 316 and 304 used in the tests was less than 0.5 μm.

ACKNOWLEDGEMENTS

The authors express their mention of gratitude to CONAHCYT (National Council of Humanities, Sciences and Technologies, Mexico), for the financial support destined for this work through the program Postdoctoral Stays by Mexico. Gratitude is extended to the Universidad Michoacana de San Nicolás de Hidalgo in Mexico, for the support received for the development of the present work.

REFERENCES

[1] Peckner, D. and Bernstein, I.M. (1977). Handbook of Stainless Steels, Part 6: The Applications of Stainless Steels, McGraw-Hill Book Company.
[2] Lula, R.A. (1986). Stainless Steel, American Society for Metals.
[3] Beddoes, J. and Parr, J.G. (1999). Introduction to Stainless Steels, 3rd edition, ASM International, Materials Park, OH, USA.
[4] Lo, K.H., Shek, C.H. and Lai, J.K.L. (2009). Recent developments in stainless steels. Materials Science and Engineering: R: Reports, 65(4-6), pp. 39–104. DOI: 10.1016/j.mser.2009.03.001.
[5] Wand, D., Jia, R., Kumseranee, S., Punpruk, S. and Gu, T. (2021). Comparison of 304 and 316 stainless steel microbiologically influenced corrosion by an anaerobic oilfield biofilm consortium. Engineering Failure Analysis (122) 105275. DOI: 10.1016/j.engfailanal.2021.105275.
[6] San Marchi, C., Michler, T., Nibur, K.A. and Somerday, B.P. (2010). On the physical differences between tensile testing of type 304 and 316 austenitic stainless steels with internal hydrogen and in external hydrogen, International Journal of Hydrogen Energy, 35, pp. 9736–9745. DOI:10.1016/j.ijhydene.2010.06.018.
[7] Lopes, F.A., Morin, P., Oliveira, R., Melo, L.F. (2006.) Interaction of Desulfovibrio desulfuricans biofilms with stainless steel surface and its impact on bacterial metabolism, J. Appl. Microbiol. 101(5), pp. 1087–1095. DOI: 10.1111/j.1365-2672.2006.03001.x.
[8] Wang, Z., Paschalidou, E.M., Seyeux, A., Zanna, S., Maurice, V. and Marcus, P. (2019). Mechanisms of Cr and Mo enrichments in the passive oxide film on 316L austenitic stainless steel, Front. Mater. 6. DOI: 10.3389/fmats.2019.00232.
[9] Hong, S.G. and Lee, S.B. (2004) The tensile and low-cycle fatigue behavior of cold worked 316L stainless steel: influence of dynamic strain aging. International Journal of Fatigue, 26 (8), pp. 899–910. DOI:10.1016/j.ijfatigue.2003.12.002.
[10] He, C., Tian, R.H., Liu, Y.J., Li, J.K. and Wang, Q.Y. (2015). Ultrasonic Fatigue Damage Behavior of 304L Austenitic Stainless Steel Based on Micro-plasticity and Heat Dissipation. Journal of Iron and Steel research, international, 22 (7), pp. 638-644. DOI: 10.1016/S1006-706X(15)30051-0.
[11] Grigorescu, A., Hilgendorff, P.M., Zimmermann, M., Fritzen, C.P. and Christ, H.J. (2018). Fatigue behaviour of austenitic stainless steels in the VHCF Regime, Fatigue of Materials at Very High Numbers of Loading Cycles, 1, pp. 49-71. DOI:10.1007/978-3-658-24531-3_3.
[12] Vincent, L., Le Roux, J.C. and Taheri, S. (2012). On the high cycle fatigue behavior of a type 304L stainless steel at room temperature, International Journal of Fatigue, 38, pp. 84–91. DOI:10.1016/j.ijfatigue.2011.11.010.
[13] Takahashi, K. and Ogawa, T. (2008). Evaluation of Giga-cycle Fatigue Properties of Austenitic Stainless Steels Using Ultrasonic Fatigue Test, Journal of Solid Mechanics and Materials Engineering, 2(3), pp. 366-373. DOI: 10.1299/jmmp.2.366.
[14] Klusák, J., Kozákova, K., Fintová, S. and Seitl, S. (2022). Fatigue lifetimes of 1.4306 and 1.4307 stainless steels subjected to ultrasonic loading, Procedia Structural Integrity, 42, pp. 1369–1375. DOI: 10.1016/j.prostr.2022.12.174.
[15] Klusák, J., Kozákova, K., Jambor, M. and Seitl, S. (2023). Fatigue behavior of DIN 1.4307 and DIN 1.4306 stainless steels under high frequency loading, Procedia Structural Integrity, 43, pp. 142–147. DOI: 10.1016/j.prostr.2022.12.249.
[16] Brickner, K.G. and Defilippi, J.D. (1977). Mechanical Properties of Stainless Steels at Cryogenic Temperatures and at Room Temperature, Handbook of Stainless Steels, McGraw-Hill Book Company.
[17] La Paloma compañia de metals. (2023.) Stainless steel, Material Technical Sheet. Available at: https://www.lapaloma.com.mx/lapaloma_metales/acero_inoxidable_z1.pdf